Active Control Damping With The Use Of Voice Coil Actuators

Giada Cardellino

Technical University of Darmstadt, System Reliability, Adaptive Structures, and Machine Acoustics SAM, Otto-Berndt-Straße 2, 64287 Darmstadt, Germany

Tobias Melz

Technical University of Darmstadt, System Reliability, Adaptive Structures, and Machine Acoustics SAM,
Otto-Berndt-Straße 2, 64287 Darmstadt, Germany
Fraunhofer-Instituts für Betriebsfestigkeit und Systemzuverlässigkeit LBF, Bartningstaße 47, 64289 Darmstadt,
Germany

Robert Feldmann

Technical University of Darmstadt, System Reliability, Adaptive Structures, and Machine Acoustics SAM, Otto-Berndt-Straße 2, 64287 Darmstadt, Germany

Christian Adams

Graz University of Technology, Institute of Fundamentals and Theory in Electrical Engineering, Professorship for Acoustics and Environmental Noise, Inffeldgasse 16c, Graz, 8010, Austria

Francesco Franco, Giuseppe Petrone and Sergio De Rosa

University of Naples "Federico II", Department of Industrial Engineering, pasta-Lab, Via Claudio 21, 80125, Napoli, Italy

I. Introduction

Vibrations, inherent in a variety of mechanical and structural systems, pose significant challenges in the aerospace industry due to their potential effects on performance, reliability, and safety. These oscillations may originate from external forces, inherent material properties, or operational conditions, affecting not only aerospace but also other sectors such as automotive, civil engineering, and industrial machinery. Addressing this complex issue, various techniques of vibration control have been developed, with active vibration control gaining importance in recent times within the aeronautical context. Active control of vibration involves dynamically manipulating a system's behavior in real-time to mitigate or suppress undesirable vibrations. In contrast to passive methods relying on damping elements, active control utilizes feedback mechanisms and actuators to actively counteract vibrations as they occur. This dynamic approach allows for precise and adaptive adjustments, holding the potential to optimize performance under varying conditions, especially crucial in the dynamic field of aerospace engineering [1]. Comparisons between passive and active methods for the vibration control were also performed in terms of uncertainty with simple mathematical linear models [2]. The primary components of an active vibration control system include sensors for measuring vibrations, a controller for processing sensor data, and actuators for applying corrective forces or moments to the structure. By continually monitoring and adjusting in real-time, active control systems effectively reduce vibrations, enhance system stability, and prolong the lifespan of critical components, all of which are paramount considerations in the design and operation of aerospace vehicles. The subject of active vibration control is well established and in continuous development: recently, several studies have been analysed and carried out from both an experimental and numerical point of view: some are reserved for the buckling control of thin-section structures subjected to compressive loads [3]; other approaches have also been considered to evaluate deterministic data in the field of active and passive vibration isolation [4].

In conjunction with the concept of active vibration control, it is becoming increasingly necessary and important to characterize a structure from the point of view of damping in the aerospace industry. Damping, a crucial aspect in structural vibrations, significantly affects the dynamic response of the structures. Recent years have seen an upsurge in the importance of damping within the context of similitude theory. The theory of the similitude has a fundamental significance in solid mechanics, allowing conclusion to be drawn regarding the vibration behaviour of a structure without needing the full-scale testing. In the field of the similitude theory, the original structure is defined as *parent*, while the scaled structure is defined as *replica* or *avatar*, depending on the degree of similitude with the original

system. If the dynamic and kinematic characteristics of the original system are preserved, and its geometric shape remains unchanged, the resulting model, differing only in size, will exhibit complete similitude and can be defined as a replica; on the contrary case, for distorted similitude, the model is defined as an avatar. An introduction to the finite similitude is provided by Davey *et al.*: first, the possibility that geometric similarity could have been broken was in-depth explored [5], paying attention also to nonlinear dynamic structural systems, which make the problem of scaling and scale laws in solid mechanics more complex [6]. The approach has also been defined and extended to the case of anisotropy characterized by thin-walled structures [7]. Other studies to develop scaling laws have been focused on different approaches: a modal approach as starting point has been considered for the SAMSARA (Similitude and Asymptotic Models for Structural-Acoustic Research and Applications) [8], power laws and a first order sensitivity analysis have been utilized for the SIMSALABIM (Similitude and Sensitivity Analysis for Laboratory vibro-Acoustics and Basic Investigations on Model-scaling) [9]. In the field of the similitude with the damping the aim is to understand whether it is possible to derive scaling laws through which the dynamic behavior of a structure with different damping characteristics than the starting system can be predicted.

This paper presents an investigation into actively controlling damping in simple structures like plates. An introduction to control strategies and the definition of active damping control is provided in Section II. The theory of thin plates is described, and the related theoretical results are presented in Section III. Section IV outlines a numerical approach considered as the starting point for the experimental phase. Section V describes the experimental setup, including the various components, and presents some preliminary results. Finally, conclusions and future applications are outlined.

II. Control strategies and active damping

Two different approaches are considered for the disturbance rejections: feedback control and forwards control [5]. The most used one, in the field of active damping, is the feedback approach, which principle is represented in Fig. 1.

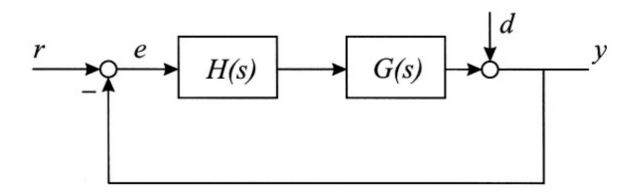


Fig. 1 Principle of feedback control [5]

The output of the system y is compared with the reference input r and the error signal e = r - y is passed into a compensator H(s) and applied to the system G(s). For lightly damped structures, feedback control serves a specific purpose: active damping. The aim of active damping is to modify the inherent damping of a structure, for instance, by increasing it to mitigate the impact of resonant peaks on the structure's response. This purpose is summarised by Equation (1):

$$\frac{y(s)}{d(s)} = \frac{1}{1 + GH}.\tag{1}$$

According to Equation (1) the goal is persuaded when GH >> 1 near the resonances. For monitoring a system with active damping control, proper type and location for a set of sensor are required focusing on the interference of the sensor or actuator with the overall system. Once the sensors and actuators have been selected, numerical models can be constructed to evaluate the modal behaviour of the structure and to understand whether the actuators and sensors can be ignored in the experimental phase as they do not interfere with the performance of the control system. This design procedure is described in Fig. 2 [5].

In the area of actuators, particular types of actuators have been chosen for the intended purpose, which are voice coil actuators represented in Fig. 3. They represent the application of the *Lorentz-Force-Principle*: the force of a current carrying wire in the magnetic field of a permanent magnet is proportional to the field strength and the current. A change of the direction of the current causes also the force to reverse; therefore voice coil motors are bidirectional actuators, both rotatory and linear ones. The current I flowing in the coil produces the force F_{VCA} given by Equation (2), in which the force sensitivity K_F of the actuator depends on the position x if the cylinder along the axis.

$$F_{VCA} = K_F(x) \cdot I. \tag{2}$$

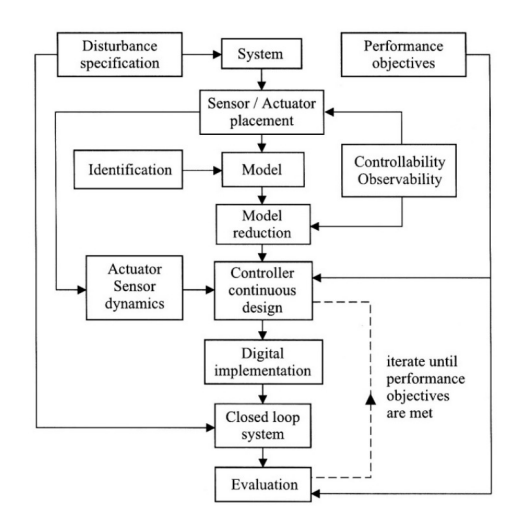


Fig. 2 Design procedure flow chart

The force F_{VCA} represents the excitation in the dynamic system considered for the experiment.

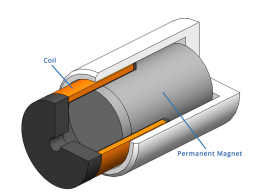


Fig. 3 Voice coil actuator

III. Theoretical background

The idea behind the use of two voice coil actuators is the one for which this shift phase can guarantee a certain amount of different damping into the original plate. The damping of a system can be influenced by various factors such as boundary conditions and mass distribution. Boundary conditions play a crucial role in determining how energy dissipates within a system [6]. Different boundary conditions can lead to different modes of vibration and, consequently, affect damping characteristics. For example, fixed boundaries may result in higher damping compared to free or sliding boundaries. The distribution of mass within a structure also affects damping. In systems with non-uniform mass distribution, certain regions may exhibit higher damping due to increased energy dissipation through internal friction or other mechanisms. Conversely, a more uniform mass distribution might result in more evenly distributed damping characteristics across the structure. Additionally, damping can be influenced by factors such as material properties and external forces acting on the system. This amount of different damping, that can be induced by multiple factors, changes the dynamic of the original plate, called *parent*, and can define a *N* plates with another damping and some geometry, called *avatars*. The idea of the active control of damping is to characterize, using the same aluminum rectangular plate, different avatars with different levels of damping. In the study the following plates listed in the Table 1 have been considered:

	Parent	Avatar 1	Avatar 2	Avatar 3	Avatar 4
Nomenclature	P	A1	A2	A3	A4
Loss factor η	2%	2.5%	3%	3.5%	4%

Table 1 Different configurations of theoretical models

The overall structural damping values considered in the Table 1 are guideline values and used for a general overview of the results. In the experimental phase, which is the most complex, the goal is to understand, starting from the initial value of structural damping of an aluminium plate of approximately $\eta = 2\%$ what is the maximum level of structural damping achievable. The geometry of the plate is kept and is a = 0.870 m, b = 0.620 m, $h = 5 \cdot 10^{-3}$ m.

A theoretical approach, referred to as Kirchhoff's thin-plate method, can be solved in the case of simply-supported boundary condition. This method assumes that plane sections normal to the mid-surface before deformation remain plane and normal to the mid-surface after deformation. Additionally, the thickness of the plate does not change during bending. For a simply-supported rectangular plate subjected to harmonic excitation, the frequency response function can be evaluated with the Kirchhoff-Love plate theory used to analyze the behavior of thin plates under bending and stretching. The Kirchhoff-Love plate theory results in a fourth-order partial differential equation governing the plate's deformation which describes the relationship between the bending moments, shearing forces, and applied loads on the plate. The general form of the Kirchhoff-Love plate equation can be written as:

$$D\nabla^4 w(x, y, t) + m \frac{\partial^2 w(x, y, t)}{\partial t^2} + p(x, y, t) = 0.$$
 (3)

Where: -w(x, y, t) is the deflection of the plate at point (x, y) and time t. $-\nabla^4$ denotes the biharmonic operator. -D is the flexural rigidity of the plate. -p(x, y, t) represents the applied distributed or concentrated load on the plate. The solution of the Equation (3) is:

$$w(P_R, P_S; \omega) = F(\omega) \sum_{i=1}^{N_M} \frac{\Phi_i(P_R)\Phi_i(P_S)}{\mu[(\omega_i^2 - \omega^2) + j\eta_i\omega_i^2]},$$
(4)

with

$$\mu = \frac{\rho_s abh}{4}.\tag{5}$$

In the Equation (4): $-\Phi_i, \omega_i, \eta_i, \mu_i$ are, respectively, the *ith* mode shape, natural frequency, modal damping and generalised mass, $-F(\omega)$ is the force amplitude, j the imaginary unit and i the mode index, $-\rho_s$ is the structural density and h is the plate thickness. The force $f(P_S,t)$ is considered as a punctual load acting at the *source* point P_S through the Kronecker delta function $\delta: f(P_S,t) = F(\omega)\delta(S_0 - S)e^{j\omega t}$.

IV. Numerical data-base construction

This section outlines the numerical procedure, which serves as a preliminary phase to the experimental work. This iterative numerical method is essential for enhancing the understanding of key control parameters, such as speed, input forces, and required current, in preparation for the experimental phase. By using numerical simulations, this procedure provides preliminary results and builds a database to support the experimental study. The experimental phase is inherently more complex due to the influence of real-world environmental factors. The construction of the numerical database is based on the following points:

- 1) A Finite Element Model of the laboratory plate is constructed. The laboratory plate is the rectangular plate a = 0.870 m, b = 0.620 m, $h = 5 \cdot 10^{-3} \text{ m}$, with free-free boundary conditions;
- 2) A Modal Analysis is performed on the described plate to assess its vibrational behavior in terms of modal shapes and natural frequencies;
- 3) A Frequency Analysis is set up on the same numerical model: in the frequency analysis, a number N_c of control points (arbitrary) is defined, where ideally, in the experimental model, the coil-moving actuators are connected, and a number N_c of points where the frequency response is measured.
 - Initially, it is hoped to conduct experimental frequency analysis up to rather high frequencies $f_{max} \simeq 1000$ Hz, so the number of points where the frequency response is measured will also be high, ranging from $10 < N_r < 20$. The number of control points where force is applied N_c (corresponding ideally to the actuator positions) will initially be higher than the experimental one (hence, only two actuators are considered).
 - Transfer functions $H(\omega)$ between all considered points, both control and response, are calculated. The number of obtained transfer functions will be equal to $N_c \times N_r$.
 - Once the transfer functions $[H]_i$ database is obtained, the inverse problem is addressed: in other words, it is necessary to understand the vibration field that the actuators must introduce to achieve a more or less

damped response \rightarrow objective function; the objective function is the result of an inverse and not quadratic problem.

- Defined the *objective function*, the control law with which to control and drive the actuators can be obtained. The result obtained will be linked to the ideal case of:
 - 1) hypothesis of system linearity;
 - 2) Validity of the superposition principle.
- 4) All the steps defined in the point 3) can be repeated changing the position of the control points (voice coil actuators point) according a procedure which is called "position optimization" or reducing the number of control points and response control to build a new data sheet.
- 5) Once the force system that the actuators must apply is obtained, it is possible to check the product's technical data-sheet for the performance curve, usually expressed in Force [N]/Current [A]. For instance, if a constant excitation force spectrum is assumed and a different force spectrum is obtained, it becomes possible to understand the current profile required to drive the actuator.
- 6) When the current law is defined backward, it is necessary to understand if the power amplifier can ensure that current. If it cannot, one must consider a lower input force.

Taking into account all the considerations listed, it is possible to understand how actuators and power amplifier are able to operate in the real case. From the mathematical point of view the iterative procedure described is reported below. The response vector is obtained from a numerical model with a damping value that is the one that experimentally wants to reached: for example, $\eta = 2.5\%$. This vector is a function of the frequency domain in the third dimension. For simplicity of representation this dependency in the third dimension can be ignored and the vector can be written as a column vector $1xN_r$ with N_r number of response points:

$$\vec{x}_{\eta=2.5\%} = \begin{bmatrix} x_1 \\ x_2 \\ \vdots \\ x_{N_r} \end{bmatrix}. \tag{6}$$

The frequency response matrix is obtained from the numerical results with an original damping $\eta = 2\%$. This frequency response matrix is, as for the response vector, a tensor in the third dimension depending on the angular frequency vector ω . In the 2-D case this frequency response matrix has the dimension $N_c x N_r$ with N_c number of control points defined as the point in which the system of force, or in an equivalent way the system of voice coil actuators, is applied.

$$\bar{\bar{H}}_{\eta=2\%} = \begin{bmatrix} H_{1,1} & H_{1,2} & \dots & H_{1,N_r} \\ H_{2,1} & H_{2,2} & \dots & H_{2,N_r} \\ \vdots & \vdots & \vdots & \vdots \\ H_{N_c,1} & H_{N_c,2} & \dots & H_{N_c,N_r} \end{bmatrix}.$$
(7)

The unknown vector is the force system vector needed by the model with initial damping assumed to be $\eta=2\%$ to obtain the displacement vector at the damping $\eta=2.5\%$ and the maximum desirable damping values. It should be noted that in the general case, since the number of response points and the number of control points are not coincident, the unknown vector of the force system will have a different dimension from the known vector. This means that the problem is not directly invertible and the inversion requires an approximation. The direct problem can be written in an implicit form as in Equation (8):

$$\frac{\vec{x}_{\{\eta=2.5\%\}}}{\text{known vector}} = \frac{\bar{\bar{H}}_{\{\eta=2\%\}}}{\text{known vector}} \cdot \vec{F}_{\{\eta=2\%\}} .$$
(8)

The non-quadratic inverse problem to solve is written in explicit form as:

$$\begin{bmatrix} F_{1} \\ F_{2} \\ \vdots \\ F_{N_{c}} \end{bmatrix}_{\{\eta=2\%\}} = \begin{bmatrix} H_{1,1} & H_{1,2} & \dots & H_{1,N_{r}} \\ H_{2,1} & H_{2,2} & \dots & H_{2,N_{r}} \\ \vdots & \vdots & \vdots & \vdots \\ H_{N_{c},1} & H_{N_{c},2} & \dots & H_{N_{c},N_{r}} \end{bmatrix}_{\{\eta=2\%\}}^{-1} \cdot \begin{bmatrix} x_{1} \\ x_{2} \\ \vdots \\ x_{N_{r}} \end{bmatrix}_{\{\eta=2.5\%\}} . \tag{9}$$

The third dimension is omitted for simplicity of representation: the third dimension represents the angular frequency ω . The problem expressed by the Equation (9) can be solved considering mathematical approximations and methods for the inversion of the rectangular matrix (tensor) \bar{H} by calculating its pseudo-inverse matrix. The problem expressed by Equation (9) can be written for each value of damping $\hat{\eta}$ wants to be reached experimentally: the numerical results will be obtained with the force spectrum needed to obtain the specific amount of damping, as already mentioned, represents only a data-base construction to have any idea of the entity and magnitude of the main quantities will be effectively involved in the experimental phase. Assuming that the problem expressed in Equation (9) is derived by considering an initial system with a damping of $\eta=2\%$, and applying a uniform and constant force spectrum across all control points, the solution to the inverse problem — expressed in terms of the amplitude and phase of the excitation vector at each control point — will remain consistent and the same for each control point (because in input the control force was unitary and the same). For this specific scenario, a number of control points $N_c=5$ is considered, and the results for one representative control point is reported. Figures [4 - 7] depict the amplitude and phase spectrum of the force required for the plate with damping $\eta=2\%$ at one control point, corresponding to the position of the voice coil actuator in the experimental setup.

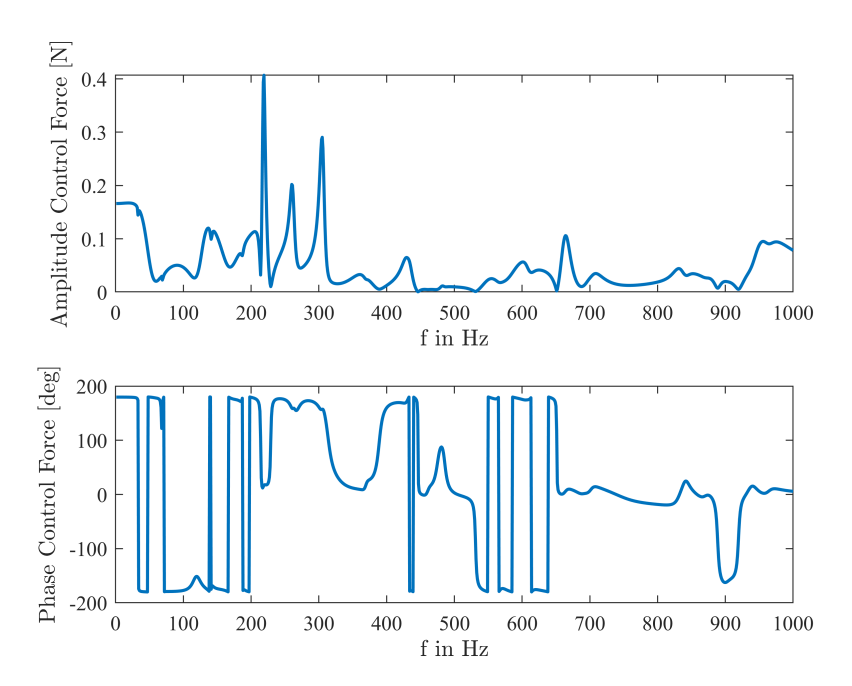


Fig. 4 Solution for the inverse problem given by Equation (9) - system of excitation for a damping $\hat{\eta} = 2.5\%$

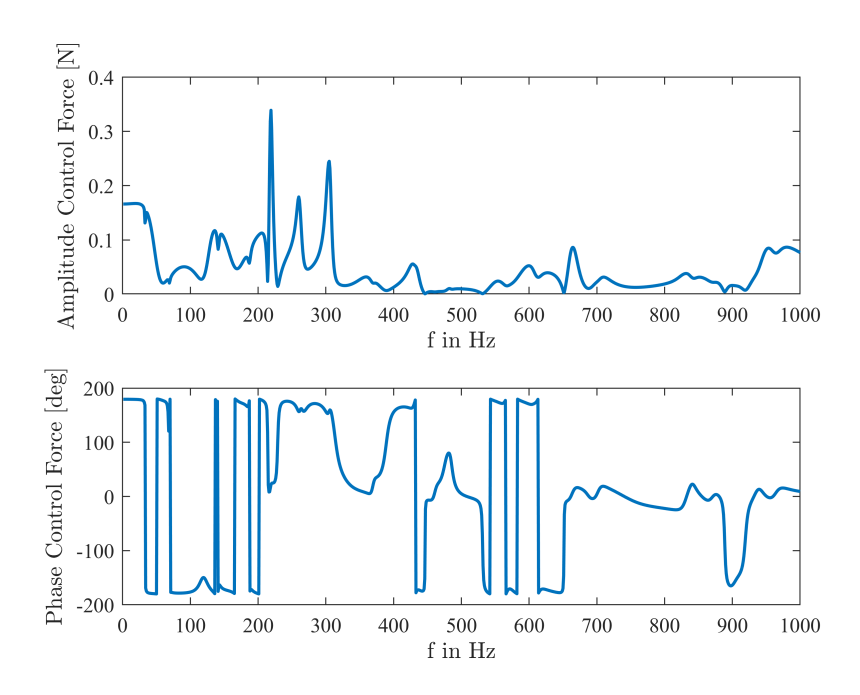


Fig. 5 Solution for the inverse problem given by Equation (9) - system of excitation for a damping $\hat{\eta} = 3\%$

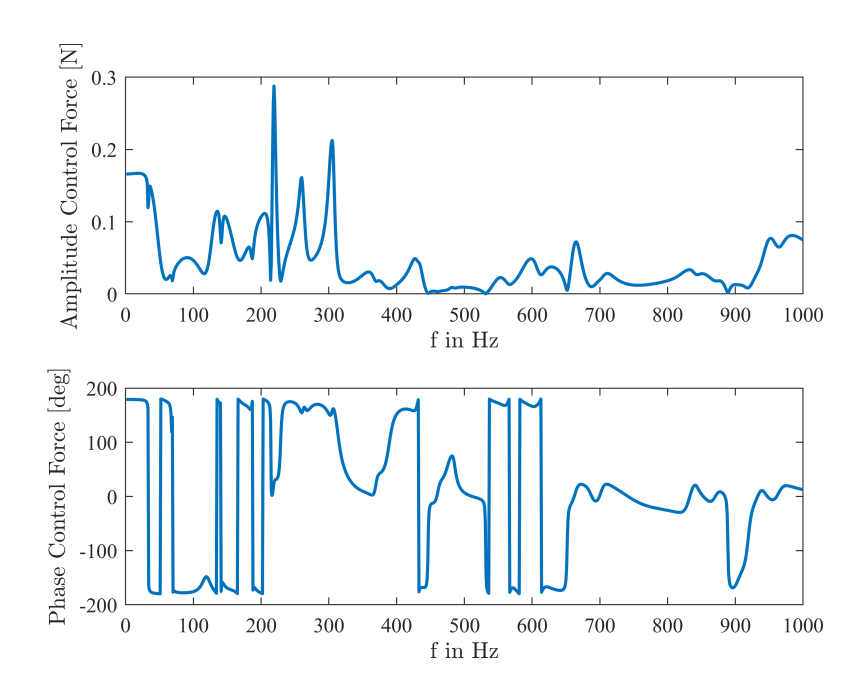


Fig. 6 Solution for the inverse problem given by Equation (9) - system of excitation for a damping $\hat{\eta} = 3.5\%$

They show the spectrum, in amplitude and phase, of the excitation that must be applied at one of the control points of the original system with damping η in order to obtain equivalent damping, without the aid of active control systems, equal to $\hat{\eta}$. As can be seen, for damping values from $\hat{\eta}=2.5\%$ to $\hat{\eta}=4\%$, the behavior of the forcing spectrum, both in magnitude and phase, is similar. Increasing the target damping value, it can be noted that, with the same trend, the amplitude function in frequency assumes lower peak values in the frequency range between f=200 Hz and f=300 Hz.

A verification of the inverse problem setup has been performed by applying Equation (9), where the pseudo-inverse

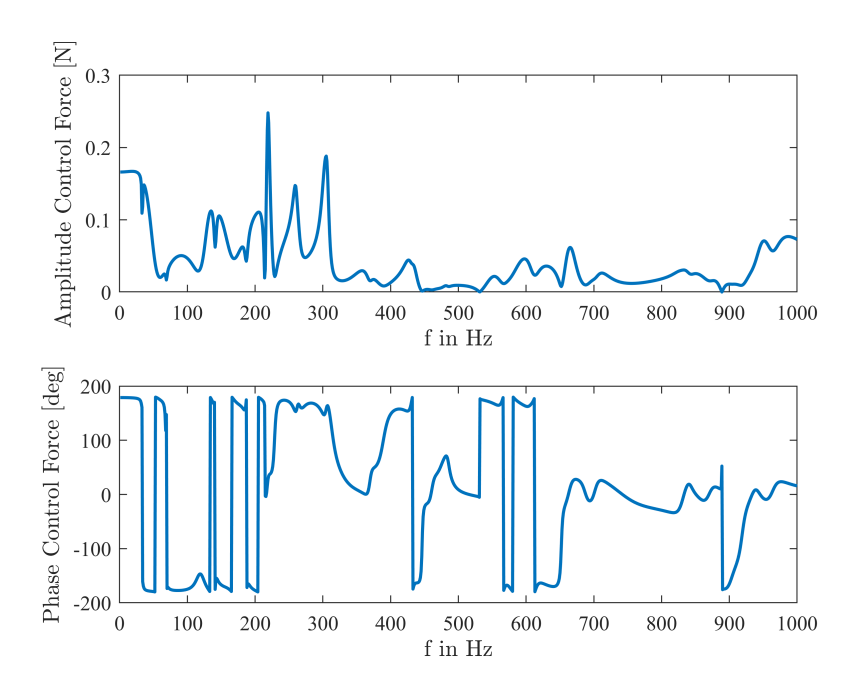


Fig. 7 Solution for the inverse problem given by Equation (9) - system of excitation for a damping $\hat{\eta} = 4\%$

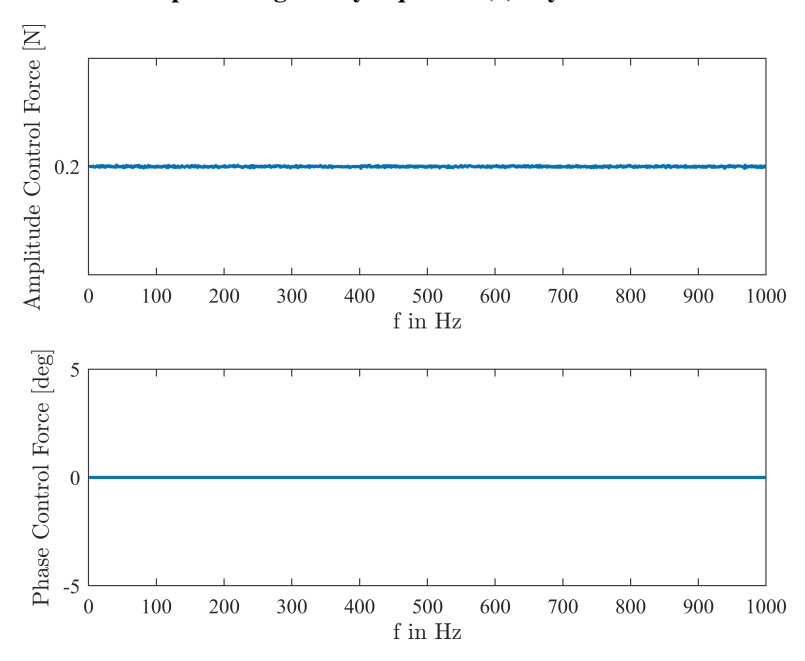


Fig. 8 Solution for the inverse problem given by Equation (9) - verification for the case $\hat{\eta} = \eta = 2\%$

problem is solved for a displacement obtained as if the goal were to achieve an equivalent damping equal to the original $\eta=2\%$. In this specific case, it is expected to obtain a force spectrum at one of the control points with a magnitude equal to the input force considered in the numerical model of the equivalent system divided by the number of control points N_c , under the assumption of linearity and superposition of effects as shown in the Fig. 8. The numerical procedure considered in this section is better explained with the flow-chart in Fig. 10. The phase representation of the force systems for different damping values is also depicted with a polar plot in Fig. 9.

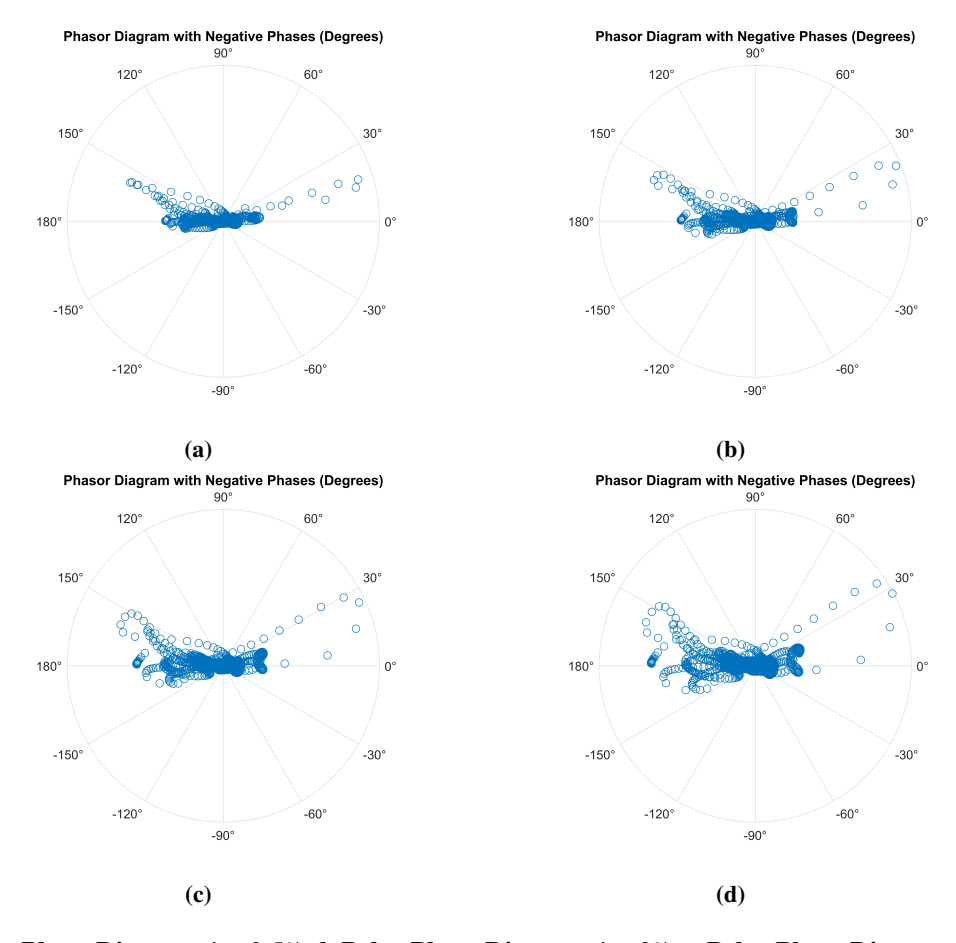


Fig. 9 a Polar Phase Diagram $\hat{\eta}=2.5\%$, b Polar Phase Diagram $\hat{\eta}=3\%$, c Polar Phase Diagram $\hat{\eta}=3.5\%$, d Polar Phase Diagram $\hat{\eta}=4\%$

V. Experimental setup

This section provides a description of the experimental preparations and essential components required for the texts execution. The setup includes a rectangular aluminum plate, two moving coil actuators and dSpace components, crucial to evaluate the frequency response of the plate. The rectangular aluminium plate has the following dimensions: length a = 0.870 m, width b = 0.620 m and thickness $b = 5 \cdot 10^{-3}$ m. The boundary conditions are those of free-free plate implemented experimentally by suspending the plate from an aluminium beam. A significant challenge in the experimental configuration involved ensuring the stability of the voice coil actuators to prevent unintended movements or forces resulting from vibrations or minor shifts. To enhance stability, clamping rings matching the diameter of the voice coil actuators are introduced. These rings serve as attachment points for the actuators and are connected to the tripods via threads, ensuring a secure linkage. To account for decoupling from the floor, elastic springs are incorporated into the setup. The mechanical properties of the aluminum plate are described in the Table 2.

Young Modulus	$E = 69 \cdot 10^9 \text{ Pa}$		
Density	$\rho = 2810 \text{ Kg/m}^3$		
Poisson Modulus	0.33		
Structural Damping	2%		

Table 2 Mechanical Properties Aluminum 6069 T3

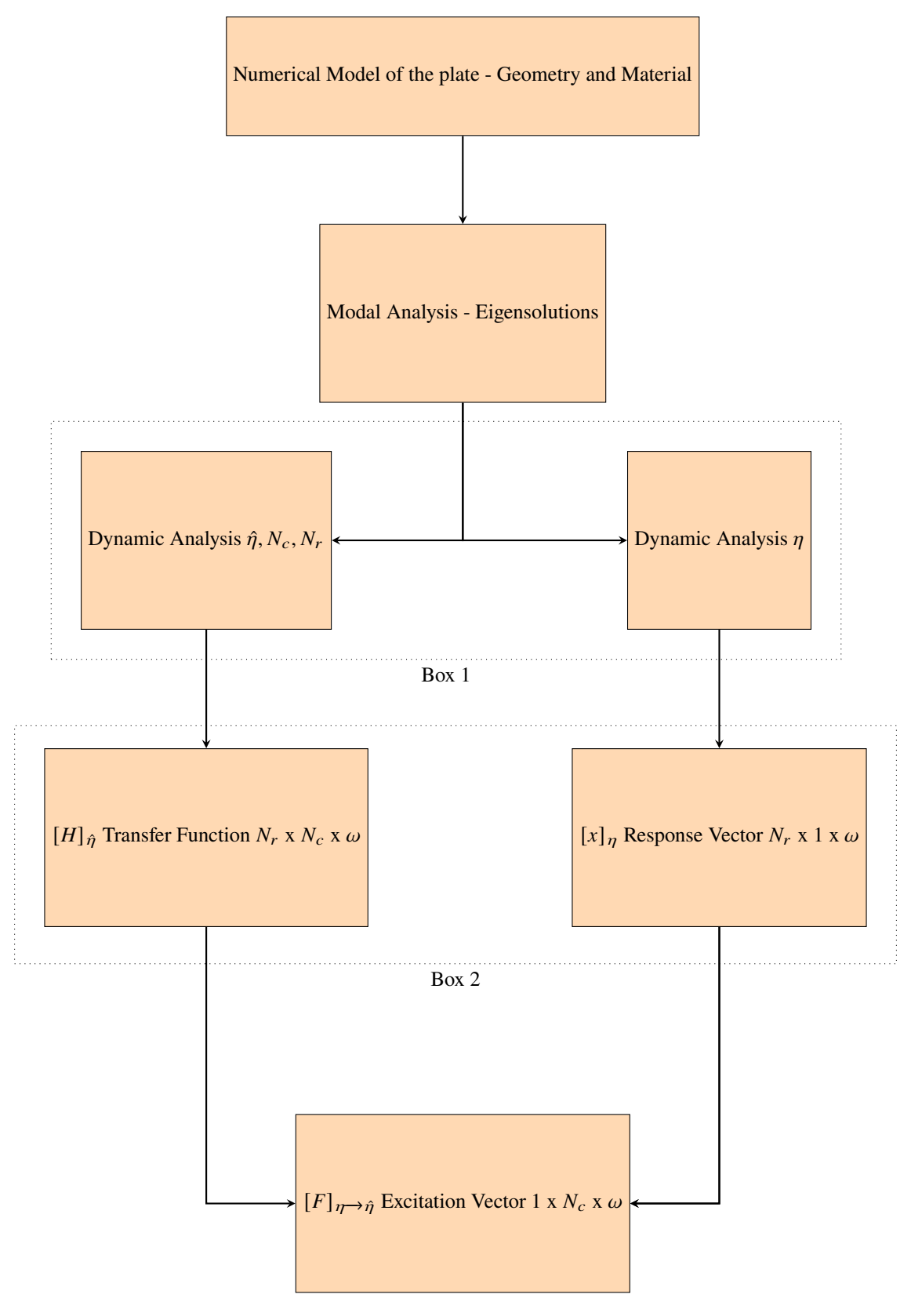


Fig. 10 Flow-chart for the numerical data base

The voice coil actuators are described in the Table 3 and represented in the Fig. 11.

External Diameter	$\Phi_e = 63.1 \text{ mm}$		
Internal Diameter	$\Phi_i = 50 \text{ mm}$		
Resistance	$R_{20}=3.7~\Omega$		
Inductance	1.8 mH		
Force Constant	F = 14 N/A		
Velocity	14 Vs/m		
Current	$I_{100} = 2.3 \text{ A}$		

Table 3 Geometry and Properties VCAs



Fig. 11 Voice Coil Actuators

The experimental setup in the laboratory is below reported: the aluminium plate is suspended from a beam and connected to the Voice coil actuators. The experiments, carried out in an iterative, trial-and-error phase, aim to



Fig. 12 Experimental setup in the laboratory

understand which avatars can be obtained by progressively changing the current intensity and stroke of the voice coil actuators. Before starting the experiments with active control and the use of dSPACE, several preliminary experimental steps are considered. These preliminary steps consist of several successive experiments:

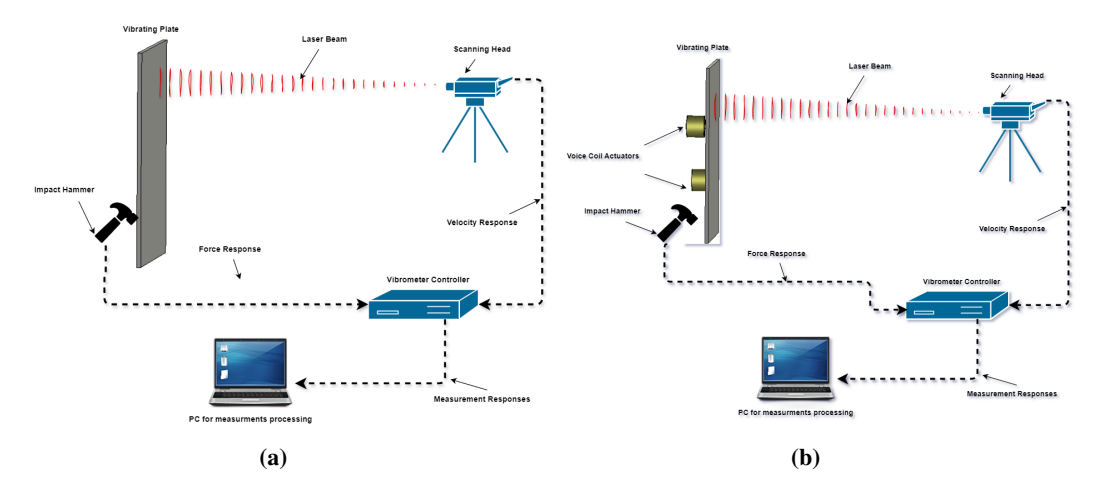


Fig. 13 a Experimental Setup with Modal Hammer, b Experimental Setup with Modal Hammer and Voice Coil Actuators

- 1) The first experiment involves evaluating the damping of the aluminum plate without the aid of mechanisms that could already slightly modify it. To achieve this, the plate is excited with a Modal Hammer and the response in terms of velocity is measured at three points on the plate both in the time and frequency domains.
- 2) Subsequently, the voice coil actuators are attached to the plate through an impedance sensor but kept turned off, and the Modal Hammer is again used as the excitation system; the response is again measured with a Laser Doppler Vibrometer at three points on the plate. The transition from step 1 to step 2 involves understanding if the additional mass due to the attachment of the voice coil actuators causes a slight increase in damping.
- 3) In the third phase, the voice coil actuators are used as the excitation system in an open-loop scheme without control.
- 4) In the fourth and more complex final phase, the control system is included in a closed-loop scheme that simultaneously modifies the excitation of the voice coil actuators.

The experimental phases are reported in the Fig 13.

VI. Conclusions

In summary, this project seeks to actively modify the internal damping of an isotropic structure to control vibrations. The primary emphasis is on addressing the challenge of determining the maximum achievable frequency within the experimental setup. This parameter is significantly influenced by various mechanical and design aspects of the voice coil actuators, including current, stroke, and force. It is essential to recognize that while the theoretical approach suggests an "unlimited" maximum frequency, practical implementation demands thorough evaluation.

The mechanical and design parameters of the voice coil actuators play a crucial role in defining the upper frequency limit, requiring careful consideration in the experimental setup. Additionally, it is crucial to underscore that the theoretical models being considered serve as conceptual frameworks. The actual damping values attainable in the experimental scenario must undergo evaluation and calculation through an iterative process.

To implement this iterative approach, we will establish a closed-loop system using dSpace hardware. This setup will enable systematic adjustments and refinements to optimize the internal damping of the isotropic structure. Through these iterations, the project aims to bridge the gap between theoretical expectations and real-world experimental outcomes, ultimately contributing to the advancement of active vibration control systems.

VII. Copyright Statement

The authors confirm that they, and/or their company or organization, hold copyright on all of the original material included in this paper. The authors also confirm that they have obtained permission, from the copyright holder of any third party material included in this paper, to publish it as part of their paper. The authors confirm that they give permission, or have obtained permission from the copyright holder of this paper, for the publication and distribution of

this paper as part of the ICAS proceedings or as individual off-prints from the proceedings.

References

- [1] Fuller, C., Elliot, S., and Nelson, P., "Active Control of Vibration," Vol. 1st Edition, 1996.
- [2] Platz, R., and Enss, G., "Comparison of Uncertainty in Passive and Active Vibration Isolation," *Model Validation and Uncertainty Quantification*, Vol. 3, No. Conference Proceedings of the Society for Experimental Mechanics Series, 2015, pp. 15–25.
- [3] Schaeffner, M., Platz, R., and Melz, T., "Active buckling control of compressively loaded beam-columns and trusses," *Methods and Technologies for Mastering Uncertainty*, 2021, pp. 343–351.
- [4] Platz, R., "Approach to Assess Basic Deterministic Data and Model Form Uncertaint in Passive and Active Vibration Isolation," *Mastering Uncertainty in Mechanical Engineering*, 2021, pp. 208–223.
- [5] Davey, K., Darvizeh, R., Golbaf, A., and Sadeghi, H., "The breaking of geometric similarity," *Internation Journal od Mechanical Sciences*, Vol. 187, No. 105925, 2020.
- [6] Davey, K., Atar, M., Sadeghi, H., and Darvizeh, R., "The scaling of nonlinear structural dynamic system," *Internation Journal od Mechanical Sciences*, Vol. 206, No. 106631, 2021.
- [7] Davey, K., Sadeghi, H., Adams, C., and Darvizeh, R., "Anisotropic scaling for thin-walled vibrating structures," *Journal of Sound and Vibration*, Vol. 537, No. 117182, 2022.
- [8] Rosa, S. D., Franco, F., and Meruane, V., "Similitudes for the structural response of flexural plates," *Journal of Mechanical Engineering Science*, Vol. 230(2), 2016, pp. 174–188.
- [9] Adams, C., Bös, J., Slomski, E., and Melz, T., "Scaling laws obtained from a sensitivity analysis and applied to thin vibrating structures," *Mechanical System and Signal Processing*, Vol. 110, 2018, pp. 590–610.